Lamb waves in phononic crystal slabs with square or rectangular symmetries

T. Brunet, Jerome O. Vasseur, Bernard Bonello, Bahram Djafari-Rouhani, Anne-Christine Hladky

Lamb waves in phononic crystal slabs with square or rectangular symmetries

Cite as: J. Appl. Phys. **104**, 043506 (2008); https://doi.org/10.1063/1.2970067
Submitted: 11 April 2008 • Accepted: 19 June 2008 • Published Online: 19 August 2008

Thomas Brunet, Jérôme Vasseur, Bernard Bonello, et al.

Lamb waves in phononic crystal slabs with square or rectangular symmetries

Thomas Brunet,[1] Jérôme Vasseur,[2] Bernard Bonello,[1,a)] Bahram Djafari-Rouhani,[2] and Anne-Christine Hladky-Hennion[2]
[1]*Institut des NanoSciences de Paris, Université Pierre et Marie Curie Paris 6, UMR CNRS 7588, 140 Rue de Lourmel, 75015 Paris, France*
[2]*Institut d'Electronique de Microélectronique et de Nanotechnologies, UMR CNRS 8520, Avenue Poincaré, Cité Scientifique, 59652 Villeneuve d'Ascq Cedex, France*

(Received 11 April 2008; accepted 19 June 2008; published online 19 August 2008)

We report on both numerical and experimental results showing the occurrence of band gaps for Lamb waves propagating in phononic crystal plates. The structures are made of centered rectangular and square arrays of holes drilled in a silicon plate. A supercell plane wave expansion method is used to calculate the band structures and to predict the position and the magnitude of the gaps. The band structures of phononic crystal slabs are then measured using a laser ultrasonic technique. Lamb waves in the megahertz range and with wave vectors ranging over more than the first two reduced Brillouin zones are investigated. © *2008 American Institute of Physics*. [DOI: 10.1063/1.2970067]

I. INTRODUCTION

A phononic crystal (PC) is made of a periodic arrangement of inclusions embedded into a matrix material with contrasted elastic properties. As for the PCs, which are its optical counterpart, the band structures of these composite structures may present under certain conditions absolute band gaps where the propagation of elastic waves is forbidden whatever the direction of propagation of the incident wave.[1] They have received a great deal of attention since the beginning of the 1990s, owing to their potential applications as sound insulators for wave filtering[2] or waveguiding.[3,4] While most of the works were initially devoted to bulk PC i.e., composite materials of infinite extent along the three spatial directions, slabs of PCs have been the subject of several studies during the last few years. Indeed, these structures are well suited to confine and to guide the elastic energy in between the free surfaces of the slab. Moreover, frequency gaps for both symmetric and antisymmetric Lamb modes have been theoretically predicted[5–9] and actually observed[10–13] in slabs of two-dimensional (2D) PCs. Note that this geometry allows for a fine tuning of both the gap magnitude and the central frequency through proper choices of the material constituents and of the geometrical parameters such as the filling fraction f and the ratio h/a, where h and a are the thickness of the slab and the lattice constant, respectively.

In this work, we applied a numerical scheme based on a plane wave expansion (PWE) of the equations of motion along three orthogonal directions to calculate the band structures of silicon plates patterned with 2D air hole arrays. Indeed, due to the huge contrast in the elastic properties of air and of the solid matrix, the PWE methods developed to date fail to compute accurately the band structures of such patterned plates.[5] This method overcomes these convergent concerns and allows for an accurate computation of the dispersion curves whatever the lattice symmetry and the shape of the holes.

Then, we have validated our approach by comparing the numerical results to the experimental data. To this end, we used a noncontact technique to measure the dispersion curves of Lamb waves propagating in air/silicon PC slabs. We have investigated PCs with two types of lattice symmetry, namely, the square and the centered rectangular lattices. In both cases, the horizontal component of the wave vector $\mathbf{k}$ lies along more than the first two Brillouin zones. We have also examined the influence of the filling factor on the results derived from both approaches.

PWE methods are generally based on the assumption that the 2D periodic lattice has infinite extents along two directions, at least. Actually, the samples used in the experiments always have finite sizes. This could be at the origin of unwanted effects that we analyze in the last part of this paper.

II. MODEL AND THEORETICAL RESULTS

In the course of the numerical calculations of the band structures of air holes/silicon PC slabs, the slabs are assumed to be of thickness h along the x_3 axis of the Cartesian coordinate system $(0,x_1,x_2,x_3)$ ($\mathbf{e_1}$, $\mathbf{e_2}$, and $\mathbf{e_3}$ are unit vectors along the x_1, x_2, and x_3 axes, respectively) and of the infinite extent in the $(x_1 0 x_2)$ transverse plane. The holes of square shape are drilled parallel to the x_3 axis and placed periodically along a square array or a centered rectangular network with various filling fractions. The origin 0 of the Cartesian coordinate system is located at the center of an inclusion. Due to the periodicity in the transverse plane, one may define a 2D primitive unit cell in the plane perpendicular to the holes where primitive vectors are depicted in Fig. 1. This allows one to define a 2D reciprocal space for both arrays of inclusions. For the square lattice of period a, the primitive vectors of the 2D reciprocal space are given as $\mathbf{b_1}:(2\pi/a,0)$

a)Electronic mail: bernard.bonello@insp.jussieu.fr.

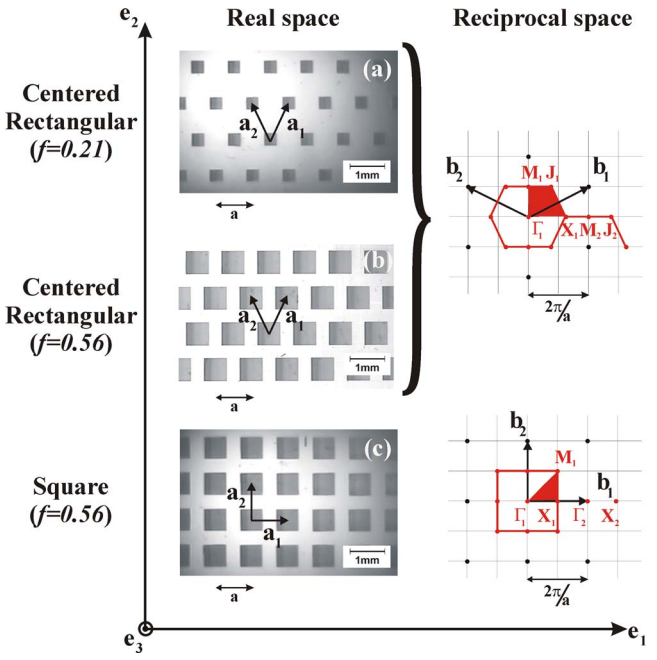

FIG. 1. (Color online) Left panel: images of the three phononic structures under study defined by the primitive vectors in real space (arrows). Centered rectangular arrays with $f=0.21$ (a) and $f=0.56$ (b) and a square array with $f=0.56$ (c). Right panel: schematic representation of the first (red lines) and of the irreducible (shaded area) Brillouin zones defined by primitive vectors in the reciprocal space (arrows). The coordinates of points Γ_1, X_1, M_2, and J_2 for the centered rectangular lattice are, respectively, (0,0), $(5\pi/4a,0)$, $(2\pi/a,0)$, and $(11\pi/4a,0)$. Coordinates of points Γ_1, X_1, Γ_2, and X_2 in the square lattice are (0,0), $(\pi/a,0)$, $(2\pi/a,0)$, and $(3\pi/a,0)$, respectively.

and $\mathbf{b_2}:(0,2\pi/a)$. Thus, the irreducible Brillouin zone is of triangular shape and the highest symmetry points are denoted as Γ_1, X_1, and M_1. The centered rectangular lattice is deduced from the square lattice by simply translating by $a/2$ along $\mathbf{e}_1$, one row of inclusions over two. This yields the primitive vectors in the 2D reciprocal space $\mathbf{b_1}:(2\pi/a,\pi/a)$ and $\mathbf{b_2}:(-2\pi/a,\pi/a)$. In this case, the irreducible Brillouin zone is tetragonal and the highest symmetry points are labeled Γ_1, X_1, J_1, and M_1.

The band structures were computed using a supercell (SC)-PWE method. In this method, the PC plate is sandwiched between two slabs of thickness d made of a fictitious low impedance material (LIM) with very low density and very high speeds of sound modeling vacuum. This allows us to define a three-dimensional SC whose basis in the $(x_1 0 x_2)$ plane includes that of the 2D primitive unit cell of the array of inclusions and whose height along the vertical axis of unit vector $\mathbf{e_3}$ is $l=h+2d$. This SC is periodically repeated along the three spatial directions, and the equations of propagation are Fourier transformed. This implies to consider a third component, along the $\mathbf{e_3}$ axis, of the primitive vectors of the reciprocal space to be equal to $2\pi/l$. Due to their very low impedance in comparison to that of the phononic slabs, the LIM forbids the interaction between the vibrational modes of neighboring periodically repeated PC plates. As we showed in previous papers,[7] our SC-PWE method is an efficient and reliable numerical tool for computing the band structures of PC plates made of air holes drilled in a solid matrix. It was also noticed that recently, another numerical work[8] reported a slightly different PWE method. It consists in considering vacuum layers with zero mass density and elastic constants as surrounding media. Both these corroborating methods do not require writing explicitly the boundary conditions on the free surfaces, therefore alleviating some numerical difficulties such as the computation of pseudomodes without physical meaning.[5]

The SC-PWE results for a 200 μm thick silicon plate, patterned with a centered rectangular and a square array of air holes displayed in Figs. 2(a) and 2(b) and Fig. 2(c), respectively. In the calculations, the lattice constants and the filling fractions were those of the samples we used in the experiments described below, i.e., $h/a=0.2$, $f=0.21$, or $f=0.56$, for the centered rectangular symmetry and $f=0.56$ for the square symmetry. For a direct comparison between the computed band structures and the experimental dispersion curves, we have calculated the band structures for $\mathbf{k}$ vectors lying along more than the second reduced Brillouin zone. More specifically we considered the $\mathbf{k}$ vectors of components k_1 and k_2 in the transverse plane with k_1 larger than $2\pi/a$ and $k_2=0$. The component k_3 of the wave vector along the x_3 axis has been fixed equal to 0. It was shown[5] that another value of k_3 at the range of $[0,\pi/l]$ does not significantly modify the numerical results.

We show in Fig. 2 the results for propagation along the path Γ_1-X_1-M_2-J_2 in the centered rectangular lattice and along Γ_1-X_1-Γ_2-X_2 in the square array. Note that the vibrational modes in the second Brillouin zone (X_1-M_2 and M_2-J_2 for the centered rectangular lattice; X_1-Γ_2 and Γ_2-X_2 for the square lattice) could be brought back to the first Brillouin zone through simple translations by vectors $\mathbf{b_2}$ (centered rectangular) and $-\mathbf{b_1}$ (square).

One notes that these band structures do not exhibit absolute band gaps but only local gaps especially for the lower order antisymmetric Lamb mode A_0 (see Table I). Absolute band gaps in such air holes/solid PC plates would require thicker plate and higher filling fractions.[7,9]

III. EXPERIMENTS

Three silicon plates (~200 μm thick) were patterned by anisotropic chemical etching, with air hole arrays drilled throughout (see Fig. 1). In each case, the rows of inclusions were parallel to the crystallographic directions [100] and [010] of silicon with a ratio $h/a=0.2$. We used a laser ultrasonic setup to measure the band structures of these PCs.[12] Our experimental technique is based on the laser generation and detection of acoustic pulses with a broad spectrum. Broadband acoustic pulses were generated at the surface of the sample by focusing light pulses issued from a frequency-doubled (532 nm) Q-switched neodymium doped yttrium aluminum garnet through a cylindrical lens. The line shaped spot was about 5 mm long and 70 μm across. In all the experiments described in this article, the excitation zone was located a few millimeters ahead of the PC itself, in a region of the sample free from any air inclusion. The time dependence of the surface displacements was recorded at regularly spaced distances from the acoustic source using a Michelson interferometer whose light source was a He–Ne laser. One

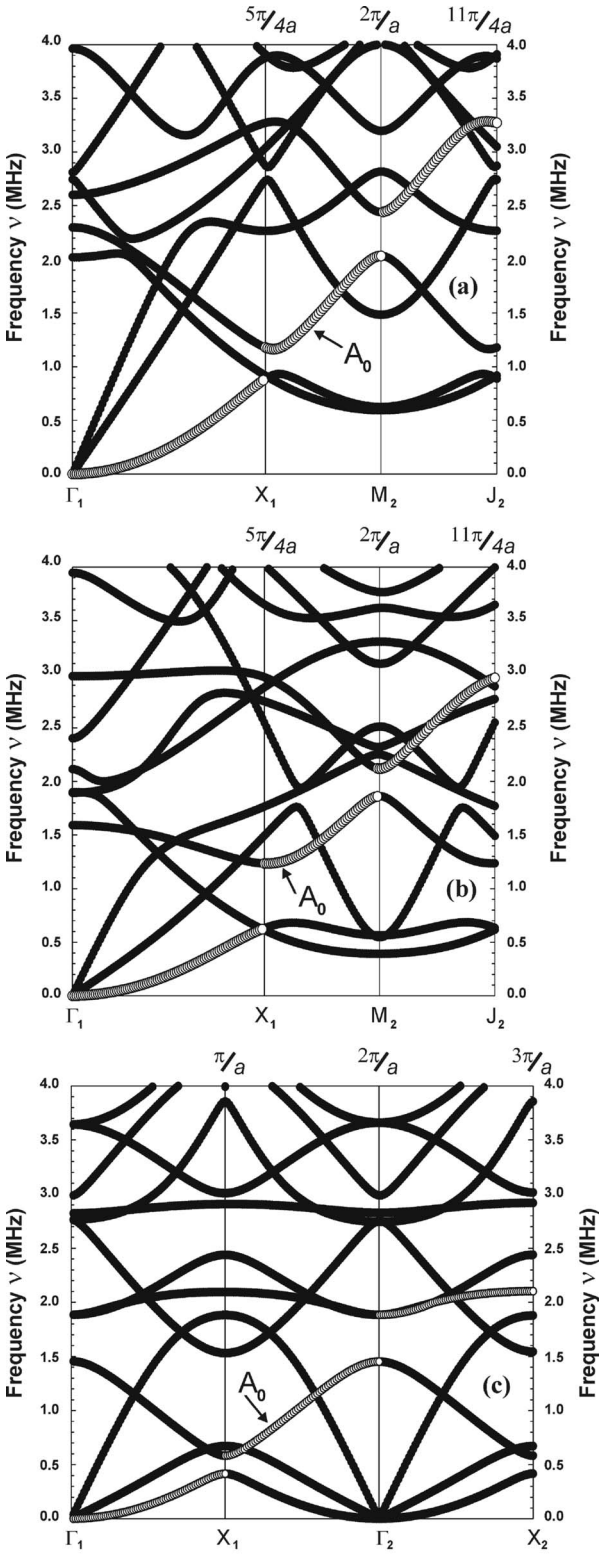

FIG. 2. Band structures of patterned silicon plates ($h/a=0.2$) for the centered rectangular array with $f=0.21$ (a) and $f=0.56$ (b) and the square array with $f=0.56$ (c) of air holes. The open circles represent the lower order antisymmetric mode A_0. The quantities on the top are for the modulus of the wave vector along the $\mathbf{e_1}$ axis.

beam of the interferometer was focused on the sample (acting as one of the mirrors of the interferometer), whose spot size was ~15 μm, whereas the reference beam was reflected by an actively stabilized mirror. The interference pattern was collected by a high-speed photodiode and then digitized at

TABLE I. Numerical and experimental values for both position ν and magnitude $\delta\nu$ of the gaps at the edges of the first and second Brillouin zones for the different cases studied here: centered rectangular array ($f=0.21$ and $f=0.56$) and square array ($f=0.56$).

		ν_1	$\delta\nu_1$	ν_2	$\delta\nu_2$
CR (0.21)	N	1.03	0.30	2.24	0.21
	E	1.05	0.20	2.25	0.25
CR (0.56)	N	0.92	0.61	1.99	0.26
	E	0.90	0.50	1.95	0.3
S (0.56)	N	0.50	0.16	1.67	0.43
	E	0.50	0.15	1.65	0.5

100 Msamples s^{-1} by a digital oscilloscope. Both the cylindrical lens and the sample were mounted on translation stages in such a way that the probe beam could be scanned across the sample with a precision of about 1 μm. This noncontact technique allowed us to record the displacement field at any point at the surface of the sample and to hence resolve fine details of the interaction of the acoustic waves with the PC. Note that this interferometric method is only sensitive to the normal component of the displacements but not to the in-plane components.

We deduced the dispersion curves of the PC slabs by performing a time-space Fourier transform of the data. We were able to investigate Lamb waves with wave numbers ranging from 0 (Γ in the reciprocal space) to 7000 m^{-1}, beyond the critical point M_2 in the reciprocal space of the centered rectangular array or beyond the point Γ_2 in the reciprocal space of the square network (Fig. 1). The Fourier magnitudes were resolved with accuracies of $\delta\nu=0.05$ MHz for the frequency and $\delta k=300$ m^{-1} for the wave number. The results are displayed in Figs. 3(a) and 3(b) (centered rectangular lattice) and Fig. 3(c) (square lattice). Since our detection scheme is based on a Michelson interferometer, it is only sensitive to the out-of-plane component of the ultrasonic waveform. This is the reason why we could only detect the lower order antisymmetric mode A_0, which has a large out-of-plane component and can therefore be easily observed by the current laser ultrasonic setup. On the contrary, the symmetric mode S_0, while actually excited as well as A_0, cannot be detected. Indeed, in the vicinity of Γ (i.e., at low k and low frequency), S_0 is longitudinally polarized.

We have reported the experimental results in Fig. 3 where the amplitudes of the time-space Fourier transforms appear in a logarithmic color scale. Band gaps clearly open in the antisymmetric branch A_0 for $k=5\pi/4a$ and $k=2\pi/a$ (centered rectangular [Figs. 3(a) and 3(b)]) or $k=\pi/a$ and $k=2\pi/a$ (square lattice [Fig. 3(c)]). We have also reported, as white dots in Fig. 3, the dispersion curves of A_0 deduced from the calculations described above [Figs. 2(a)–2(c)]. The agreement is excellent for both geometries and whatever the filling fraction is ($f=0.21$ or $f=0.56$), showing that our numerical approach is well suited to predict the elastic behavior of PC slabs with finite thickness.

One can note, in the investigated area [Figs. 3(b) and 3(c)], the large deviation of the dispersion curve A_0 of the PC plates with $f=0.56$ from one of the homogeneous silicon slab

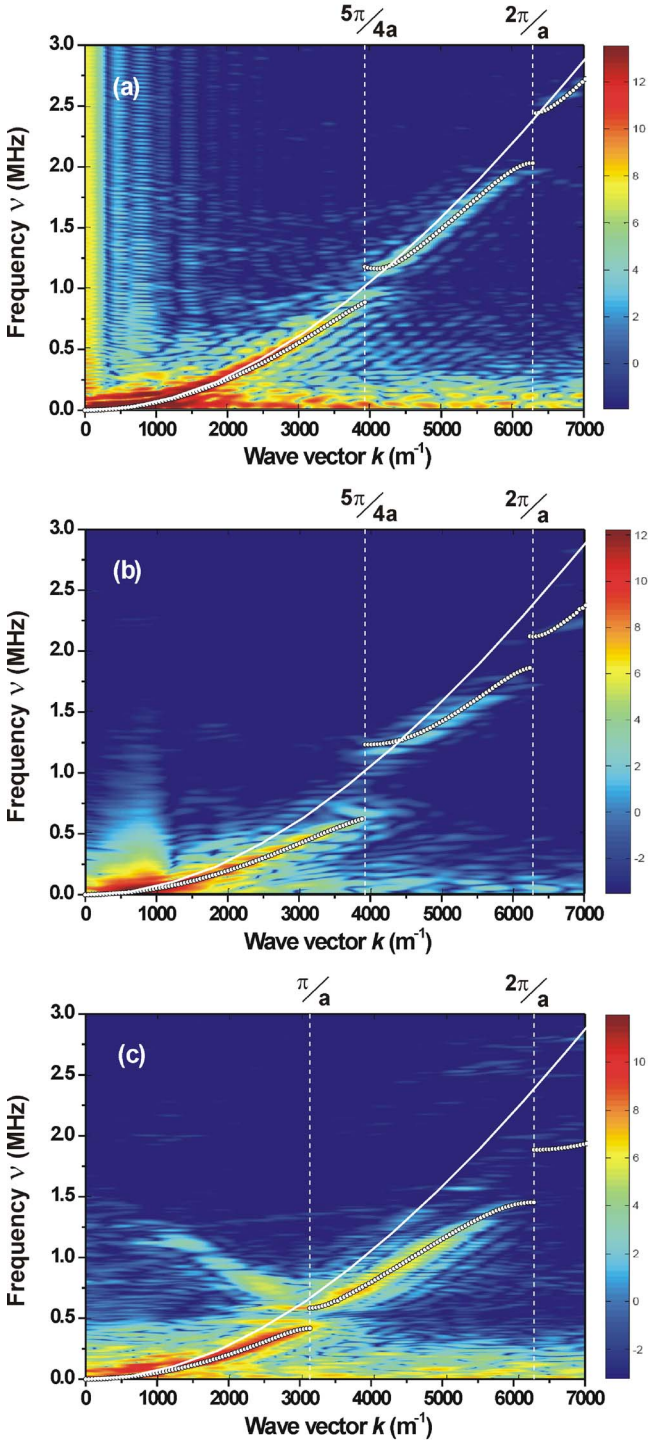

FIG. 3. (Color online) Experimental dispersion curves along Γ_1-X_1 of the phononic plates deduced through the 2D fast Fourier transform from the measured displacement fields. The color scale is logarithmic. Filling fractions are $f=0.21$ (a) and $f=0.56$ (b) for the centered rectangular array; $f=0.56$ for the square array (c). The white dots refer to the numerical band structures shown in Fig. 2. The solid lines are for the calculated Lamb mode A_0 propagating along the crystallographic axis [100] of a 200 μm thick silicon homogeneous plate.

(full line) with the same thickness ($h=200$ μm). This is due to the high filling fraction of the slab decreasing significantly its effective elastic constants and consequently the wave velocity in the PC. On the contrary, the dispersion curve overlays quite well for the lattice owing to a low filling fraction ($f=0.21$). It is also interesting to notice that, in the case of the centered rectangular symmetry, the midfrequency ν_1 of the first band gap is about the same whatever the filling fraction is (see Table I).

In addition to the dispersion curves of mode A_0, a branch with a negative slope is clearly observable at the range $[0,\pi/a]$ in Fig. 3(c) (i.e., along Γ_1-X_1). To understand the nature of this mode, one should remember that our broadband excitation scheme allows for both the excitation and the detection of elastic waves with wave vectors outside the first reduced Brillouin zone. Therefore, folded modes are not expected to appear in the 2D Fourier transforms of the displacement fields; we rather attribute this branch to the signature of elastic waves reflected by the edges of the sample propagating backwards. This is further supported by the measured amplitude of this mode which is about two orders of magnitude less than the one measured along the branch at the range $[\pi/a,2\pi/a]$ (i.e., X_1-Γ_2) with the same frequencies. Indeed, these backward waves are detected after they have traveled over a distance twice as long as the forward waves and have therefore undergone a strong attenuation through diffusion by the air hole inclusions.

IV. SUMMARY

We have presented a combined theoretical and experimental study of Lamb waves in 2D PC plates made of square holes drilled in silicon. We have analyzed the effects of the geometry of the array of holes and of the filling factor on the lower order antisymmetric A_0 Lamb mode. The results derived from both approaches are in remarkable agreement and show that local gaps occur for the A_0 mode. Considering the same filling factor, the centered rectangular array leads to larger gaps than the square network. Using the same reliable tools, an investigation of localized modes associated with the existence of structural defects such as rectilinear waveguides or cavities should be the subject of future works.

[1] J. O. Vasseur, B. Djafari-Rouhani, L. Dobrzynski, M. S. Kushwaha, and P. Halevi, J. Phys.: Condens. Matter **6**, 8759 (1994).
[2] M. Kafesaki, M. M. Sigalas, and N. Garcia, Phys. Rev. Lett. **85**, 4044 (2000).
[3] T. Miyashita and C. Inoue, Jpn. J. Appl. Phys., Part 1 **40**, 3488 (2001).
[4] T. Miyashita, Meas. Sci. Technol. **16**, R47 (2005).
[5] B. Bonello, C. Charles, and F. Ganot, Ultrasonics **44**, e1259 (2006).
[6] A. Khelif, B. Aoubiza, S. Mohammadi, A. Adibi, and V. Laude, Phys. Rev. E **74**, 046610 (2006).
[7] J. O. Vasseur, P. A. Deymier, B. Djafari-Rouhani, and Y. Pennec, Proceedings of the International Mechanical Engineering Congress and Exposition, Chicago, Illinois, 2006 (ASME, Chicago, 2006), p. 13353; J. O. Vasseur, P. A. Deymier, B. Djafari-Rouhani, Y. Pennec, and A-C. Hladky-Hennion, Phys. Rev. B **77**, 085415 (2008).
[8] Z. Hou and B. M. Assouar, Phys. Lett. A **A372**, 2091 (2008).
[9] S. Mohammadi, A. A. Eftekhar, A. Khelif, H. Moubchir, R. Westafer, W. D. Hunt, and A. Adibi, Electron. Lett. **43**, 898 (2007).
[10] J. C. Hsu and T. T. Wu, Phys. Rev. B **74**, 144303 (2006).
[11] X. Zhang, T. Jackson, E. Lafond, P. Deymier, and J. O. Vasseur, Appl. Phys. Lett. **88**, 041911 (2006).
[12] B. Bonello, C. Charles, and F. Ganot, Appl. Phys. Lett. **90**, 021909 (2007).
[13] F. L. Hsiao, A. Khelif, H. Moubchir, A. Choujaa, C. C. Chen, and V. Laude, Phys. Rev. E **76**, 056601 (2007).